

**Article**  
**Discoveries**

**Title:** Synergistic binding of bHLH transcription factors to the promoter of the maize *NADP-ME* gene used in C<sub>4</sub> photosynthesis is based on an ancient code found in the ancestral C<sub>3</sub> state

**Authors:** Ana Rita Borba<sup>1,2</sup>, Tânia S. Serra<sup>1,2</sup>, Alicja Górka<sup>1,2</sup>, Paulo Gouveia<sup>1,2</sup>, André M. Cordeiro<sup>1,2</sup>, Ivan Reyna-Llorens<sup>3</sup>, Jana Kneřová<sup>3</sup>, Pedro M. Barros<sup>1</sup>, Isabel A. Abreu<sup>1,2</sup>, M. Margarida Oliveira<sup>1,2</sup>, Julian M. Hibberd<sup>\*,3</sup>, Nelson J. M. Saibo<sup>\*,1,2</sup>

**Author information**

<sup>1</sup>Instituto de Tecnologia Química e Biológica António Xavier, Universidade Nova de Lisboa, 2780-157, Oeiras, Portugal.

<sup>2</sup>Instituto de Biologia Experimental e Tecnológica, 2780-157, Oeiras, Portugal.

<sup>3</sup>Department of Plant Sciences, Downing Street, University of Cambridge, Cambridge CB2 3EA, UK.

**\*Corresponding authors:** email: jmh65@cam.ac.uk; saibo@itqb.unl.pt.

## Abstract

C<sub>4</sub> photosynthesis has evolved repeatedly from the ancestral C<sub>3</sub> state to generate a carbon concentrating mechanism that increases photosynthetic efficiency. This specialised form of photosynthesis is particularly common in the PACMAD clade of grasses, and is used by many of the world's most productive crops. The C<sub>4</sub> cycle is accomplished through cell-type specific accumulation of enzymes but *cis*-elements and transcription factors controlling C<sub>4</sub> photosynthesis remain largely unknown. Using the *NADP-Malic Enzyme (NADP-ME)* gene as a model we tested whether mechanisms impacting on transcription in C<sub>4</sub> plants evolved from ancestral components found in C<sub>3</sub> species. Two basic Helix-Loop-Helix (bHLH) transcription factors, ZmbHLH128 and ZmbHLH129, were shown to bind the C<sub>4</sub> *NADP-ME* promoter from maize. These proteins form heterodimers and ZmbHLH129 impairs *trans*-activation by ZmbHLH128. Electrophoretic mobility shift assays indicate that a pair of *cis*-elements separated by a seven base pair spacer synergistically bind either ZmbHLH128 or ZmbHLH129. This pair of *cis*-elements is found in both C<sub>3</sub> and C<sub>4</sub> Panicoid grass species of the PACMAD clade. Our analysis is consistent with this *cis*-element pair originating from a single motif present in the ancestral C<sub>3</sub> state. We conclude that C<sub>4</sub> photosynthesis has co-opted an ancient C<sub>3</sub> regulatory code built on G-box recognition by bHLH to regulate the *NADP-ME* gene. More broadly, our findings also contribute to the understanding of gene regulatory networks controlling C<sub>4</sub> photosynthesis.

**Key words:** basic Helix-Loop-Helix, *cis*-element evolution, C<sub>3</sub> and C<sub>4</sub> photosynthesis, NADP-Malic Enzyme, PACMAD Panicoid grasses.

## Introduction

$C_3$  plants inherited a carbon fixation system developed by photosynthetic bacteria, with atmospheric carbon dioxide ( $CO_2$ ) being incorporated into ribulose-1,5-bisphosphate (RuBP) by the enzyme Ribulose Bisphosphate Carboxylase/Oxygenase (RuBisCO) to form the three-carbon compound ( $C_3$ ) 3-phosphoglycerate (Calvin and Massini 1952). However, RuBisCO can also catalyse oxygenation of RuBP, which leads to the production of 2-phosphoglycolate, a compound that is toxic to the plant cell and needs to be detoxified through an energetically wasteful process called photorespiration (Bowes et al. 1971; Sharkey 1988; Sage 2004). The oxygenase reaction of RuBisCO becomes more common as temperature increases and so in  $C_3$  plants photorespiration can reduce photosynthetic output by up to 30% (Ehleringer and Monson 1993). In environments such as the tropics where rates of photorespiration are high,  $C_4$  photosynthesis has evolved repeatedly from the ancestral  $C_3$  state (Lloyd and Farquhar 1994; Osborne and Beerling 2006). Phylogenetic studies estimate that the first transition from  $C_3$  to  $C_4$  occurred around 30 million years ago (MYA) (Christin et al. 2008; Vicentini et al. 2008; Christin et al. 2011). The ability of the  $C_4$  cycle to concentrate  $CO_2$  around RuBisCO limits oxygenation and so increases photosynthetic efficiency in conditions where photorespiration is enhanced (Hatch and Slack 1966; Maier et al. 2011; Christin and Osborne 2014; Lundgren and Christin 2016).

The evolution of  $C_4$  photosynthesis involved multiple modifications to leaf anatomy and biochemistry (Hatch 1987; Sage 2004). In most  $C_4$  plants, photosynthetic reactions are partitioned between two distinct cell types known as mesophyll (M) and bundle sheath (BS) cells (Langdale 2011). M and BS cells are arranged in concentric circles around veins in the so-called Kranz anatomy (Haberlandt 1904), which enables  $CO_2$  pumping from M to BS where RuBisCO is specifically located. Atmospheric  $CO_2$  is first converted to  $HCO_3^-$  by carbonic anhydrase (CA) and then combined with phosphoenolpyruvate (PEP) by PEP-carboxylase (PEPC) to produce oxaloacetate in the M cells. This four-carbon acid ( $C_4$ ) is subsequently converted into malate and/or aspartate that transport the fixed  $CO_2$  from M to BS cells (Kagawa and Hatch 1974; Hatch 1987). Three biochemical  $C_4$  subtypes are traditionally described based on the predominant type of  $C_4$  acid decarboxylase responsible for the  $CO_2$  release around RuBisCO in the BS: NADP-dependent Malic Enzyme (NADP-ME, e.g. *Zea mays*), NAD-dependent Malic

Enzyme (NAD-ME, e.g. *Gynandropsis gynandra* formerly designated *Cleome gynandra*) and phosphoenolpyruvate carboxykinase (PEPCK). However, recent reports suggest that only the NADP-ME and NAD-ME should be considered as distinct C<sub>4</sub> subtypes, which in response to environmental cues may involve a supplementary PEPCK cycle (Williams et al. 2012; Y. Wang et al. 2014; Rao and Dixon 2016).

The recruitment of multiple genes into C<sub>4</sub> photosynthesis involved both an increase in their transcript levels (Hibberd and Covshoff 2010) and also patterns of expression being modified from relatively constitutive in C<sub>3</sub> species (Maurino et al. 1997; Penfield et al. 2004; Taylor et al. 2010; Brown et al. 2011; Maier et al. 2011) to M- or BS-specific in C<sub>4</sub> plants (Hibberd and Covshoff 2010). Therefore, considerable efforts have been made to identify the transcription factors (TF) and the *cis*-elements they recognise that are responsible for this light-dependent and cell-specific gene expression (Hibberd and Covshoff 2010). Various studies suggest that different transcriptional regulatory mechanisms have been adopted during C<sub>3</sub> to C<sub>4</sub> evolution. One is the acquisition of novel *cis*-elements in C<sub>4</sub> gene promoters that can be recognised by TFs already present in C<sub>3</sub> plants (Matsuoka et al. 1994; Ku et al. 1999; Nomura et al. 2000), and a second possibility is the acquisition of novel or modified TFs responsible for the recruitment of genes into the C<sub>4</sub> pathway through *cis*-elements that pre-exist in C<sub>3</sub> plants (Patel et al. 2006; Brown et al. 2011; Kajala et al. 2012).

A small number of *cis*-elements found in different gene regions have been shown to be sufficient for the M- or BS-specific expression of C<sub>4</sub> genes. For example, a 41 base pair (bp) Mesophyll Expression Module 1 (MEM1) *cis*-element was identified from the *PEPC* promoter of C<sub>4</sub> *Flaveria trinervia* and shown to be necessary and sufficient for M cell-specific accumulation of *PEPC* transcripts in C<sub>4</sub> *Flaveria* species (Gowik et al. 2004). A MEM1-like *cis*-element has also been found in the C<sub>4</sub> carbonic anhydrase (*CA3*) promoter of *Flaveria bidentis* and shown to drive M cell-specific expression (Gowik et al. 2016). A second *cis*-element named MEM2 and consisting of 9 bp from untranslated regions has also been shown to be capable of directing M-specificity in C<sub>4</sub> *G. gynandra* (Kajala et al. 2012; Williams et al. 2016). Lastly, in the case of the *NAD-ME* gene from C<sub>4</sub> *G. gynandra* a region from the coding sequence generates BS-specificity (Brown et al. 2011). In contrast to these



insights into *cis*-elements that control cell-specific expression in the C<sub>4</sub> leaf, no TFs recognising these *cis*-elements have yet been identified.

To address this gap in our understanding, a bottom-up approach was initiated to identify TFs that regulate the maize gene *ZmC<sub>4</sub>-NADP-ME* (GRMZM2G085019) that encodes the Malic Enzyme responsible for releasing CO<sub>2</sub> in the BS cells. Using Yeast One-Hybrid two maize TFs belonging to the superfamily of basic Helix-Loop-Helix (bHLH), ZmbHLH128 and ZmbHLH129, were identified and functionally characterised. We show that these TFs bind two *cis*-elements synergistically and analysis of the *NADP-ME* promoters from grass species from BEP and PACMAD (Panicoideae subfamily) indicated that this regulation is likely derived from an ancestral G-box that is present in C<sub>3</sub> species.

## Results

### **ZmbHLH128 and ZmbHLH129 homeologs bind FAR1/FHY3 Binding Site *cis*-elements in the *ZmC<sub>4</sub>-NADP-ME* promoter**

To identify TFs that interact with the *ZmC<sub>4</sub>-NADP-ME* gene (GRMZM2G085019), we studied the promoter region comprising 1982 base pairs (bp) upstream of the translational start site. This region was divided into six overlapping fragments ranging from 235 to 482 bp in length (supplementary table S1) and used in Yeast One-Hybrid (Y1H). Each fragment was used to generate one yeast bait strain that was then used to screen a maize cDNA expression library. After screening at least 1.3 million colonies for each region of the promoter, two maize bHLH TFs known as ZmbHLH128 and ZmbHLH129 were identified. Both of these TFs bind the promoter between base pairs -389 and -154 in relation to the predicted translational start site of *ZmC<sub>4</sub>-NADP-ME* (fig. 1A). These interactions were confirmed by re-transforming yeast bait strains harbouring each of the six sections of the promoter with cDNAs encoding ZmbHLH128 and ZmbHLH129. Consistent with the initial findings, ZmbHLH128 and ZmbHLH129 only activated expression of the *HIS3* reporter when transformed into yeast containing fragment -389 to -154 bp upstream of *ZmC<sub>4</sub>-NADP-ME* (fig. 1B, supplementary fig. S1).

ZmbHLH128 and ZmbHLH129 possess a bHLH domain followed by a contiguous leucine zipper (ZIP) motif (fig. 1C). This bHLH domain is highly conserved between both ZmbHLHs and consists of 61 amino acids that can be separated into two functionally distinct regions. The first is a basic region located at the N-terminal end of the bHLH domain and is involved in DNA binding, and the second is a Helix-Loop-Helix region mediating dimerization towards the carboxy-terminus (fig. 1C) (Murre et al. 1989; Toledo-Ortiz et al. 2003). ZmbHLH128 and ZmbHLH129 share 91% amino acid identity (fig. 1C) and they are encoded by homeolog genes located in syntenic regions of maize chromosomes 4 and 5 (fig. 1D, supplementary table S2).

Although ZmbHLH128 and ZmbHLH129 both possess three amino acids involved in G-box binding (K9, E13, and R17) (Massari and Murre 2000; Li et al. 2006), this family of TFs has also been shown to bind to N-box (5'-CACGCG-3'), N-box B (5'-CACNAG-3') and FBS (FAR1/FHY3 Binding Site, 5'-CACGCGC-3') motifs (Sasai et al. 1992; Ohsako et al. 1994; Fisher and Caudy 1998; Kim et al. 2016). Therefore, the *ZmC<sub>4</sub>-NADP-ME* promoter was assessed for additional *cis*-elements

to which ZmbHLH128 and ZmbHLH129 might bind. A total of eight such *cis*-elements were found, consisting of two N-boxes B, two N-boxes, one G-box, two FBSs and one E-box (fig. 2A). Electrophoretic Mobility Shift Assays (EMSA) were used to test whether ZmbHLH128 and ZmbHLH129 were able to interact with each of these *cis*-elements *in vitro* (fig. 2B and C). Consistent with the Y1H findings, EMSA showed that recombinant Trx::ZmbHLH128 and Trx::ZmbHLH129 proteins caused an uplift of radiolabeled probes containing FBS *cis*-elements (probes 6, 7, and 6+7) (fig. 2C), positioned between nucleotides -389 and -154 in relation to the predicted translational start site (see fig. 1A). ZmbHLH128 also showed weak binding to probe 3 that contained a N-box *cis*-element that was not bound by ZmbHLH128 or ZmbHLH129 in Y1H (see fig. 1B), and signal intensity was similar to that observed from probe 7 (fig. 2C). We can not exclude however that relatively weak binding to probe 7 is due to it being three nucleotides-shorter than the other probes (fig. 2B). Trx alone and OsPIF14 (a bHLH known to bind the N-box motif (Cordeiro et al. 2016)) were used as negative controls (fig. 2C). The two FBS motifs, in probe 6+7, are separated by a short 7 bp spacer sequence and are found in opposite orientations (fig. 2B). The increase in band intensities detected when both *cis*-elements were combined (fig. 2C) suggests that they function synergistically. Overall, these data indicate that ZmbHLH128 and ZmbHLH129 target 21bp of DNA sequence (7bp FBS, 7bp spacer, and 7bp FBS).

### **ZmbHLH128 and ZmbHLH129 form both homo- and heterodimers and ZmbHLH129 impairs *trans*-activation by ZmbHLH128**

Because ZmbHLH128 and ZmbHLH129 bind the FBS *cis*-elements in close proximity but also possess domains mediating protein dimerization, we next investigated whether these proteins form homo- and/or heterodimers. *In vitro*, the recombinant Trx::ZmbHLH128 and Trx::ZmbHLH129 proteins formed homodimers (fig. 3A). To confirm this interaction *in vivo*, as well as to test for heterodimerization, Bimolecular Fluorescence Complementation Assays (BiFC) in maize protoplasts were performed. Whilst negative controls produced no YFP fluorescence, ZmbHLH128 and ZmbHLH129 formed both homo- and heterodimers (fig. 3B). With the exception of ZmbHLH129 homodimers whose location extended to the cytoplasm and plasma membrane, in each case YFP signal was specifically localised to the nucleus (fig. 3B). Nuclear localisation of these ZmbHLH proteins

supports their roles as transcriptional regulators.

To test the capacity of ZmbHLH128 and ZmbHLH129 to regulate transcription, transient expression assays were performed in leaves of *Nicotiana benthamiana*. The *GUS* reporter gene driven by the fragment of *pZmC<sub>4</sub>-NADP-ME* to which ZmbHLH128 and ZmbHLH129 bind was used as reporter, whilst the full-length *ZmbHLH128* and *ZmbHLH129* CDS sequences driven by the constitutive *CaMV35S* promoter were used as effectors (fig. 4A). Co-infiltration of this reporter with the ZmbHLH128 effector resulted in an increase in *GUS* activity, indicating that ZmbHLH128 can act as a transcriptional activator (fig. 4B). In contrast, ZmbHLH129 showed no intrinsic *trans*-activation activity (fig. 4C). In order to test whether the ZmbHLH128-ZmbHLH129 heterodimers had a different *trans*-activation activity from ZmbHLH128 or ZmbHLH129 homodimers, leaves were co-infiltrated with the reporter and both effectors simultaneously. Interestingly, the *trans*-activation activity observed for the ZmbHLH128 alone (fig. 4B) was lost when this TF was co-expressed with its homeolog ZmbHLH129 (fig. 4D).

#### **The G-box-based *cis*-element pair recognised by ZmbHLH128 and ZmbHLH129 in *NADP-ME* promoters operates synergistically**

To understand whether the two FBS *cis*-elements identified in the promoter of *ZmC<sub>4</sub>-NADP-ME* (see fig. 2) are associated with the evolution of C<sub>4</sub> photosynthesis, we investigated whether they are conserved in promoters of other *NADP-MEs* from C<sub>3</sub> and C<sub>4</sub> grass species. Three C<sub>3</sub> species (*Dichanthelium oligosanthes*, *Oryza sativa* and *Brachypodium distachyon*) and three C<sub>4</sub> species (*Zea mays*, *Sorghum bicolor* and *Setaria italica*) were assessed (fig. 5A). Within the C<sub>4</sub> species, *Zea mays* and *Sorghum bicolor* possess two plastidic *NADP-ME* isoforms: one that is used in C<sub>4</sub> photosynthesis (C<sub>4</sub>-*NADP-ME*, GRMZM2G085019 and Sobic.003g036200) and a second one not involved in the C<sub>4</sub> cycle (*nonC<sub>4</sub>-NADP-ME*, GRMZM2G122479 and Sobic.009g108700) (Alvarez et al. 2013; Emms et al. 2016). In contrast, *S. italica* possesses only one plastidic *NADP-ME* isoform that is used in the C<sub>4</sub> cycle (C<sub>4</sub>-*NADP-ME*, Si000645) (Alvarez et al. 2013; Emms et al. 2016).

Although in C<sub>3</sub> *B. distachyon* no homologous *cis*-elements to the FBSs in the *ZmC<sub>4</sub>-NADP-ME* promoter were detected, in *O. sativa* one G-box was found in the same position as FBS 1 from *Z. mays*. Moreover, in the other promoters, *cis*-elements that can bind bHLH proteins were present in pairs (fig. 5A). In both the C<sub>3</sub>

and C<sub>4</sub> grasses these *cis*-element pairs flank a spacer that is highly conserved in sequence and length (7 to 9 bp) (fig. 5A). The C<sub>4</sub>-*NADP-ME* promoters from *Z. mays* and *S. bicolor* share a common mutation in the third nucleotide position of the alignment (A→G) (fig. 5A). Two additional mutations are specific to *Z. mays* (the first and last nucleotides of FBS 1 and FBS 2, respectively), whilst one is *S. bicolor*-specific (C→T at the fourth position) (fig. 5A). It is possible that mutations unique to *Z. mays* or *S. bicolor* are neutral and the main impact on C<sub>4</sub>-*NADP-ME* gene expression is due to mutation in the third nucleotide in the common ancestor of *Z. mays* and *S. bicolor*. Alternatively, it is also possible that both this mutation in the last common ancestor and species-specific modifications impacted on gene expression of C<sub>4</sub>-*NADP-ME*.

To test if ZmbHLH128 and ZmbHLH129 bind the *cis*-elements identified from these additional species EMSA was performed on each *cis*-element separately as well as the *cis*-element pairs found in each *NADP-ME* promoter (fig. 5B and C, supplementary table S3). ZmbHLH128 and ZmbHLH129 showed low binding affinity for the single G-box identified in the *O. sativa* promoter (probe 13) and binding affinity was not increased by mutating the G-box to a canonical N-box (probe m13) (fig. 5B and C). This low binding affinity behaviour for single G-box *cis*-elements was consistent for all the *NADP-ME* promoters containing G-boxes (probes 5, 7, 9 and 11) (fig. 5B and C). Although both ZmbHLHs did not show binding affinity for the additional N-boxes or N-box-like alone (probes 6, 8, 10 and 12) (fig. 5B and C), when these additional motifs were acquired and formed a pair with the ancestral G-box, binding affinity was increased (probes 5+6, 7+8, 9+10 and 11+12) and led to an increased uplift compared with the G-boxes alone (probes 5, 7, 9 and 11) (fig. 5B and C). Given the similar length of probes 1, 2, 1+2, 5, 7, 9 and 11 (24 to 30 bp) (supplementary table S3), it is possible that this difference in migration of ZmbHLH-probe complexes results from the binding of bHLH to G-boxes in a lower oligomeric state (supplementary fig. S2), which based on the literature must be dimers (De Masi et al. 2011). Strong binding of *cis*-element pairs was also observed when the ancestral G-box evolved into either FBS or FeRE1 elements found in C<sub>4</sub> *Z. mays* and *S. bicolor* (probes 1+2 and 3+4) (fig. 5B and C). In the C<sub>4</sub> *Z. mays* promoter, both ZmbHLHs showed binding affinity for single FBS *cis*-elements (probes 1 and 2) in the highest oligomeric state (fig. 5B and C, supplementary fig. S2).

Since ZmbHLH128 and ZmbHLH129 showed weak binding to single *cis*-elements, we tested their binding by mutating these *cis*-elements in probes with the pairs (supplementary fig. S3). For each pair, three mutant probes were designed: two in which the two *cis*-elements were mutated individually (keeping one *cis*-element wild-type) and one in which both *cis*-elements were mutated simultaneously (supplementary table S3). Competition experiments were performed using radiolabeled wild-type probes (with *cis*-element pairs) and 200- to 400-fold excess of unlabeled wild-type and mutant probes (supplementary fig. S3). Binding of both ZmbHLHs to the labeled wild-type probes could be efficiently out-competed by unlabeled wild-type and mutant probes in which the following *cis*-elements were not mutated: FBS 1 (in *Z. mays* C<sub>4</sub>-NADP-ME, probe 1+m2-A, supplementary fig. S3A); FBS 2 (in *Z. mays* C<sub>4</sub>-NADP-ME, probe m1+2-B, supplementary fig. S3A); N-box (in *S. bicolor* C<sub>4</sub>-NADP-ME, probe m3+4-E, supplementary fig. S3B); and G-box (in *S. italica* C<sub>4</sub>-NADP-ME, probe 5+m6-G, supplementary fig. S3C; *Z. mays nonC<sub>4</sub>*-NADP-ME, probe 7+m8-J, supplementary fig. S3D; *S. bicolor nonC<sub>4</sub>*-NADP-ME, probe 9+m10-M, supplementary fig. S3E; and *D. oligosanthos* C<sub>3</sub>-NADP-ME, probe 11+m12-P, supplementary fig. S3F). These EMSA competition experiments thus confirmed binding of ZmbHLH128 and ZmbHLH129 to the *cis*-elements described above. Taken together, the results indicate that a second *cis*-element recognised by bHLH TFs is acquired in the promoters of genes encoding plastidic NADP-ME and that each *cis*-element pair operates synergistically to allow interaction with either ZmbHLH128 or ZmbHLH129 in C<sub>3</sub> and C<sub>4</sub> grasses (fig. 5, supplementary fig. S2 and S3).

Given the binding affinity *in vitro* of ZmbHLH128 and ZmbHLH129 to the G-box in the *ZmnonC<sub>4</sub>*-NADP-ME promoter (probes 7 and 7+8, fig. 5C), we tested their binding ability *in planta*. Transient expression assays were performed in leaves of *N. benthamiana* co-infiltrated with *GUS* reporter gene driven by a *ZmnonC<sub>4</sub>*-NADP-ME promoter fragment containing the *cis*-element pair G- and N-box-like (-368 to -143 bp) and the effector constructs ZmbHLH128 and ZmbHLH129 (supplementary fig. S4A). Compared with the reporter alone, co-infiltration of *ZmnonC<sub>4</sub>*-NADP-ME reporter and the ZmbHLH128 and ZmbHLH129 effectors did not impact on *GUS* activity in tobacco system (supplementary fig. S4B-D). These results suggest that although ZmbHLH128 on its own binds both the *ZmC<sub>4</sub>*-NADP-ME and *ZmnonC<sub>4</sub>*-

*NADP-ME* promoters *in vitro* (probes 1, 2, 1+2, 7 and 7+8, fig. 5B and C), this might not be the case *in planta* (supplementary fig. S4).

### **Acquisition of N-box-derived *cis*-elements in *NADP-ME* promoters facilitates ZmbHLH128 and ZmbHLH129 binding in PACMAD Panicoid grasses**

Phylogenetic analysis of the genes encoding C<sub>3</sub> and C<sub>4</sub> plastidic *NADP-ME*s reflects previously reported grass species phylogeny (fig.6A) (Grass Phylogeny Working Group II 2012). It inferred two main clades: one formed by C<sub>3</sub> BEP species (*B. distachyon* and *O. sativa*) and a second formed by C<sub>3</sub> (*D. oligosanthos*) and C<sub>4</sub> Panicoid species of the PACMAD clade (*S. italica*, *S. bicolor* and *Z. mays*) (fig.6A).

Based on the observed nucleotide modifications in *cis*-elements recognised by bHLH TFs, we propose a model relating to the recruitment of *NADP-ME* into C<sub>4</sub> photosynthesis in grasses (fig. 6B). This proposes that an ancestral G-box found in the *NADP-ME* promoter of the common ancestor of C<sub>3</sub> BEP *O. sativa* and C<sub>4</sub> Panicoid grasses has been conserved during the evolution of C<sub>4</sub> photosynthesis. However, in the Panicoideae subfamily of the PACMAD clade a second *cis*-element recognised by bHLH is present such that the *NADP-ME* gene from the C<sub>3</sub> species *D. oligosanthos* and genes encoding plastidic *nonC*<sub>4</sub>-*NADP-ME* from C<sub>4</sub> *S. bicolor* and *Z. mays* all contain a G- and N-box/N-box-like pair. In C<sub>4</sub> *S. italica* this *cis*-code has been retained in the C<sub>4</sub>-*NADP-ME*, but in *S. bicolor* and *Z. mays* the original G-box has evolved to become either a FeRE1 or a FBS element, respectively (fig. 6B). No G-box motifs are, however, present in the promoter of genes encoding cytosolic *NADP-ME* from *S. bicolor* and *Z. mays*. Overall, these results suggest that the acquisition of N-box-derived *cis*-elements have facilitated ZmbHLH128 and ZmbHLH129 binding to promoters of genes encoding plastidic *NADP-ME* in the PACMAD (Panicoideae subfamily).

## Discussion

### **ZmbHLH128 and ZmbHLH129 homeologs interact with maize C<sub>4</sub>- and nonC<sub>4</sub>-NADP-ME promoters *in vitro* showing different *trans*-activation activity *in planta***

In this study, we showed that ZmbHLH128 and ZmbHLH129 form a maize homeolog pair resulting from the recent maize whole genome duplication (WGD) event that occurred 5-12 million years ago. This WGD occurred 5-16 million years after C<sub>4</sub> photosynthesis evolved in the Andropogoneae tribe of the PACMAD clade (17-21 MYA) (Christin et al. 2008; Christin et al. 2009). As the length of exons 1 and 2 and the total number of amino acids in the mature protein of ZmbHLH128 are more similar to sorghum ortholog SbbHLH66 (supplementary fig. S5), we propose that ZmbHLH129 has diverged more from the ancestral gene. Both of these TFs bind two FBS *cis*-elements that are in close proximity in the maize C<sub>4</sub>-NADP-ME (GRMZM2G085019) promoter. Although ZmbHLH128 has been predicted *in silico* to regulate C<sub>4</sub> photosynthesis (L. Wang et al. 2014), as far as we are aware, this is the first report of its functional characterization. ZmbHLH128 alone activates *ZmC<sub>4</sub>-NADP-ME* gene expression, whilst ZmbHLH129 alone shows no *trans*-activation activity on this promoter. As the duplication event that generated ZmbHLH129 took place after the evolution of C<sub>4</sub> photosynthesis, it seems possible that this gene is not required for C<sub>4</sub> photosynthesis. ZmbHLH128 and ZmbHLH129 form heterodimers and despite ZmbHLH128 activating the expression of *ZmC<sub>4</sub>-NADP-ME* its regulatory activity is impaired by its homeolog ZmbHLH129. To explain this impairment, we hypothesise different scenarios that may occur *in vivo*: either ZmbHLH128 and ZmbHLH129 act as heterodimers and ZmbHLH128 loses its DNA binding activity when combined with ZmbHLH129 or they act as homodimers and compete directly for the same FBSs, towards which ZmbHLH129 has a higher binding affinity. The former scenario has been described for bZIP TFs from *Arabidopsis*, where bZIP63 has negative effects on the formation of bZIP1-DNA complexes probably due to conformational differences between bZIP1 homodimer and bZIP1-bZIP63 heterodimers (Kang et al. 2010). The latter scenario has been reported for the maize Dof1 and Dof2 TFs. Dof1 is a transcriptional activator of light-regulated genes in leaves, however, in stems and roots, this TF is not able to regulate those genes since the repressor Dof2 is expressed there and blocks Dof-specific *cis*-elements (Yanagisawa and Sheen 1998).



In addition to the capacity of ZmbHLH128 and ZmbHLH129 to interact with FBSs found in the maize *C<sub>4</sub>-NADP-ME* promoter, both ZmbHLHs were shown to bind *in vitro* to the promoter of maize *nonC<sub>4</sub>-NADP-ME* (GRMZM2G122479) that possesses the *cis*-element pair G- and N-box-like. *In planta*, however, ZmbHLH128 and ZmbHLH129 showed no *trans*-activation activity on this promoter. It is well known that primary DNA sequence and its structural properties are determinants of DNA binding specificity *in vivo* (Rohs et al. 2009) and so it is possible that both ZmbHLHs display increased *in vivo* binding specificity for the FBS pair in the *ZmC<sub>4</sub>-NADP-ME* promoter than for the G- and N-box-like pair in the *ZmnonC<sub>4</sub>-NADP-ME* promoter. Therefore, ZmbHLH128 seems to affect the level of expression of *NADP-ME* as it activates the *ZmC<sub>4</sub>-NADP-ME* promoter through the pair formed by two FBSs but the same trend was not observed for the *ZmnonC<sub>4</sub>-NADP-ME* promoter with the G- and N-box pair. Additionally, we hypothesise that these modifications of promoter sequences may also affect light/circadian regulation of the *ZmC<sub>4</sub>-NADP-ME* gene as FBS *cis*-elements have been described in promoters of circadian-clock-regulated and light-responsive genes (Lin et al. 2007; Li et al. 2011; Kim et al. 2016). The mutation of two close FBSs in the promoter of the circadian-clock gene EARLY FLOWERING 4 (*ELF4*) proved to be sufficient to abolish its rhythmic expression (Li et al. 2011). More broadly, our findings also contribute to the understanding of gene regulatory networks controlling *C<sub>4</sub>* photosynthesis.

### **The G-box-based *cis*-element pair present in *NADP-ME* promoters synergistically bind either ZmbHLH128 or ZmbHLH129**

We identified a *cis*-element pair recognised by bHLH that occupy homologous positions in *NADP-ME* promoters from *C<sub>3</sub>* and *C<sub>4</sub>* grasses. These *cis*-elements flank a short spacer and operate synergistically to facilitate interaction with ZmbHLH128 and ZmbHLH129. We suggest a mechanism by which these TFs may be recruited to the *cis*-elements associated with *C<sub>4</sub>* photosynthesis. We propose that one *cis*-element is sufficient to recruit a bHLH homodimer (G-box) or tetramer (N-box or FBS in promoters where the ancestral G-box is no longer present), however, the presence of a second *cis*-element in the vicinity increases bHLH binding affinity (supplementary fig. S2). It is possible that both *cis*-elements are brought together through the interaction with a bHLH tetramer formed by two dimers, which may involve DNA bending (supplementary fig. S2). Therefore, this *cis*-element pair could

operate synergistically to confer stabilisation of bHLH binding. This mechanism of TF-DNA assembly has previously been proposed for MADS-domain TFs that can bind two nearby CArG boxes through DNA looping and formation of tetrameric complexes (Theissen 2001; Theissen and Saedler 2001; Melzer and Verelst 2009; Smaczniak et al. 2012; Smaczniak et al. 2017). In this case, and consistent with our results, MADS-domain TFs were found to bind single CArG boxes either as dimers or tetramers, however, when their target gene promoters contain CArG box pairs they bind as tetramers (Smaczniak et al. 2012). It has been proposed that the probability of DNA loop formation increases with shorter distances between *cis*-elements due to the low elastic bending energy required to bring the protein dimers together (Agrawal et al. 2008). Interestingly, in all *NADP-ME* promoters assessed in this study except rice and *Brachypodium* the two *cis*-elements were found to be in close proximity, which may encourage DNA looping. In addition to the spacer length, its sequence appears highly conserved. This is consistent with evidence suggesting that nucleotides outside core *cis*-elements affect TF binding specificity by providing genomic context and influencing three-dimensional structure (Atchley et al. 1999; Martínez-García et al. 2000; Grove et al. 2009; Gordân et al. 2013). For example, Cbf1 and Tye7 are yeast bHLHs that show preference for a subset of G-boxes present throughout the yeast genome (Gordân et al. 2013). These differences in binding preferences were observed not just *in vivo* but also *in vitro* and so DNA sequences flanking core G-boxes were found to explain this differential bHLH-G-box binding (Gordân et al. 2013).

The mechanism proposed here for how bHLH TFs interact with their target *cis*-elements suggests that these DNA sequences are not randomly arranged in gene promoters and may affect how *cis*-element specificity is achieved. Indeed, in some promoters bound by bHLH TFs two or more *cis*-elements were found to be clustered. For example, two overlapping FBSs were reported in the 400 base pairs upstream of the translational start site of the gene encoding ELF4 (Li et al. 2011). Also, pairs of G- and N-boxes were found to be highly enriched in promoters targeted by the bHLH PIF1 (Kim et al. 2016). It is possible that multiple *cis*-elements serve to recruit additional TFs for *in vivo* cooperative binding.

**C<sub>4</sub> photosynthesis co-opted an ancient C<sub>3</sub> *cis*-regulatory code built on G-box recognition by bHLH transcription factors**

Finally, from this work we propose a model that summarises how molecular evolution of *cis*-elements recognised by bHLHs may relate to the recruitment of *NADP-ME* into C<sub>4</sub> photosynthesis. C<sub>4</sub> photosynthesis is an excellent example of convergent evolution (Sage et al. 2011; Christin et al. 2013) as it has evolved independently over 60 times in angiosperms (Sage et al. 2011; Sage 2016) and at least 22 times in grasses (Grass Phylogeny Working Group II 2012). How this repeated evolution has come about is not fully understood. Our model contributes to our understanding of C<sub>4</sub> evolution and is based on the following findings: first, in rice, which belongs to the BEP clade that contains no C<sub>4</sub> species, only one copy of a G-box was present in the *NADP-ME* promoter. In contrast, *cis*-element pairs recognised by ZmbHLH128 and ZmbHLH129 in *NADP-ME* promoters seem to be common in the Panicoideae subfamily of the PACMAD clade that contains independent C<sub>4</sub> lineages. For example, in the PACMAD Panicoid grasses a G- and N-box pair was identified in C<sub>3</sub> *D. oligosanthos* (Do024386) and appears to be reasonably conserved in C<sub>4</sub> species. However, in the case of the C<sub>4</sub>-*NADP-MEs* from *S. bicolor* and *Z. mays* (Sobic.003g036200 and GRMZM2G085019) these elements have diversified. Both of these grass species belong to the C<sub>4</sub> tribe Andropogoneae in which the plastidic *NADP-ME* isoform that is used in C<sub>4</sub> photosynthesis (C<sub>4</sub>-*NADP-ME*) evolved by duplication from an ancestral plastidic *NADP-ME* that still exists and is not involved in the C<sub>4</sub> cycle (*nonC*<sub>4</sub>-*NADP-ME*, Sobic.009g108700 and GRMZM2G122479) (Tausta et al. 2002; Maier et al. 2011; Alvarez et al. 2013). In contrast, C<sub>4</sub> *S. italica* together with C<sub>3</sub> *D. oligosanthos* belong to the grass tribe Paniceae in which only one plastidic *NADP-ME* isoform is known to exist (Si000645 and Do024386) (Alvarez et al. 2013; Emms et al. 2016). Surprisingly, the *cis*-element pair identified in the C<sub>4</sub>-*NADP-ME* promoter from *S. italica* (G- and N-box) was found to be closer to those occurring in the C<sub>3</sub> and *nonC*<sub>4</sub>-*NADP-ME* promoters from *D. oligosanthos*, *S. bicolor*, and *Z. mays* (G- and N-box/N-box-like) than to those occurring in the C<sub>4</sub>-*NADP-ME* promoters from *S. bicolor* and *Z. mays* (FeRE1 and N-box or FBS and FBS, respectively). A similar trend has previously been observed (Alvarez et al. 2013) and may be explained by the independent evolutionary origin of C<sub>4</sub> photosynthesis in grass tribes formed by *S. italica* (Paniceae) or *S. bicolor*/*Z. mays* (Andropogoneae).

Taken together, our findings suggest that an ancestral G-box in combination with N-box-derived *cis*-elements form the basis of the synergistic binding of either

453 ZmbHLH128 or ZmbHLH129 to *NADP-ME* promoters from PACMAD Panicoid  
 454 grasses. Nucleotide diversity in *cis*-elements recognised by bHLH TFs has been  
 455 suggested as one of the mechanisms by which these TFs are involved in complex  
 456 and diverse transcriptional activity (Toledo-Ortiz et al. 2003). We, therefore, can not  
 457 exclude the possibility that the gene encoding the plastidic NADP-ME from C<sub>3</sub> BEP  
 458 *Brachypodium distachyon* (BRADI2g05620) can also be bound by ZmbHLH128 or  
 459 ZmbHLH129 despite none of the typical *cis*-elements recognised by bHLH being  
 460 identified in the promoter. Given recent evidence indicating that the bHLH TF family  
 461 is often recruited into C<sub>4</sub> photosynthesis regulation (Huang and Brutnell 2016), we  
 462 suggest that the observed nucleotide modifications in the *cis*-element pair present in  
 463 C<sub>4</sub>-*NADP-ME* promoters from *S. bicolor* and *Z. mays* may underlie changes in bHLH  
 464 binding specificity *in vivo* and, therefore, contribute to the *NADP-ME* recruitment into  
 465 C<sub>4</sub> photosynthesis in the Andropogoneae tribe from the PACMAD clade. The  
 466 presence of a bHLH duplicate (ZmbHLH129) that seems not to be required for C<sub>4</sub>  
 467 photosynthesis and has evolved to repress the activity of its homeolog  
 468 (ZmbHLH128) is unique to maize as this homeolog gene pair resulted from the  
 469 maize WGD. Therefore, we hypothesise that the single orthologous bHLH in all the  
 470 other Panicoid species of the PACMAD clade activates C<sub>4</sub>-*NADP-ME* gene  
 471 expression. This agrees with the hypothesis that C<sub>4</sub> photosynthesis has on multiple  
 472 occasions made use of *cis*-regulators found in C<sub>3</sub> species and, therefore, that the  
 473 recruitment of C<sub>4</sub> genes was made through minor rewiring of pre-existing regulatory  
 474 networks (Reyna-Llorens and Hibberd 2017). We conclude that regulation of C<sub>4</sub>  
 475 genes can be based on an ancient code founded on a G-box present in the BEP  
 476 clade as well as the Panicoideae of the PACMAD clade. Acquisition of a second *cis*-  
 477 element recognised by bHLH in Panicoid grasses appears to have facilitated  
 478 synergistic binding by either ZmbHLH128 or ZmbHLH129. Although this G-box-  
 479 based *cis*-code has remained similar in *S. italica*, it has diverged in maize and  
 480 sorghum. Thus, different C<sub>4</sub> grass lineages may employ slightly different molecular  
 481 circuits to regulate orthologous C<sub>4</sub> photosynthesis genes.

## Materials and methods

### Plant growth conditions and collection of leaf samples

To construct the cDNA expression library, maize plants (*Zea mays* L. var. B73) were grown at 16h photoperiod with a light intensity of 340-350  $\mu\text{mol m}^{-2} \text{s}^{-1}$ , at day/night temperature of 28°C/26°C, and 70% relative humidity. Two light regimes were used: (1) nine days in 16h photoperiod; and (2) nine days in 16h photoperiod followed by a 72h dark treatment. In both experiments, sample collection was performed under 16h photoperiod. Third leaves grown in the former and latter light regimes were harvested respectively at time points covering the Zeitgeber times (ZT) -0.5, 0.5, 2h, and ZT 1, 2, 4, 8, 12, 15.5h. For isolation of maize mesophyll protoplasts, maize plants were grown for 10 days at 25°C, 16h photoperiod (60  $\mu\text{mol m}^{-2} \text{s}^{-1}$ ), and 70% relative humidity. For transient expression assays *in planta*, *Nicotiana benthamiana* (tobacco) plants were grown for five weeks at 22°C, 16h photoperiod (350  $\mu\text{mol m}^{-2} \text{s}^{-1}$ ), and 65% relative humidity. After agro-infiltration of tobacco leaves, plants were left to grow into the same growth conditions and leaf discs (2.5 cm in diameter) collected 96h post-infection.

### Generation of yeast bait strains

Yeast bait strains were generated as previously described (Ouwerkerk and Meijer 2001; Serra et al. 2013). Yeast strain Y187 (Clontech) was used to generate six bait strains carrying overlapping fragments of the *ZmC<sub>4</sub>-NADP-ME* (GRMZM2G085019) promoter cloned into the yeast integrative vector pINT1-HIS3 (Ouwerkerk and Meijer 2001) as *NotI-SpeI* or *XbaI-SpeI* fragments (supplementary table S1). The *ZmC<sub>4</sub>-NADP-ME* promoter region was defined as the 1982 bp upstream of the predicted translational start site (ATG). To assess self-activation/*HIS3* leaky expression, yeast bait strains were titrated in complete minimal medium (CM) lacking histidine, with increasing concentrations of 3-amino-1,2,4-triazole (3-AT, up to 75 mM).

### Construction of cDNA expression library

Total RNA was extracted from third leaves of maize seedlings using TRIzol reagent (Invitrogen), following the manufacturer's instructions. RNA samples from nine time points (described in 'plant growth conditions and collection of leaf samples') were pooled in equal amounts for mRNA purification using the PolyAtract mRNA Isolation

System IV (Promega). A unidirectional cDNA expression library was prepared using the HybriZAP-2.1 XR cDNA Synthesis Kit and the HybriZAP-2.1 XR Library Construction Kit (Stratagene), following the manufacturer's instructions. Four micrograms of mRNA were used for first strand cDNA synthesis. After *in vivo* excision and amplification of the pAD-GAL4-2.1 phagemid vector, this maize cDNA expression library was used to transform yeast bait strains.

### **Yeast One-Hybrid (Y1H) screening and validation**

Yeast bait strains were transformed with 1 µg of maize cDNA expression library according to Ouwerkerk and Meijer (2001) and Serra et al. (2013). At least, 1.3 million yeast colonies of each yeast bait strain transformed with the maize cDNA expression library were screened in CM -HIS -LEU supplemented with 3-AT: 5 mM (-1982 to -1524 bp), 20 mM (-389 to -154 bp, -776 to -334 bp) or 75 mM (-973 to -702 bp, -1225 to -891 bp, -1617 to -1135 bp). Plasmids from yeast clones that actively grew on selective medium were extracted. To know whether the isolated clones encoded transcription factors (TFs), the cDNA insert was sequenced and the results analysed using BLAST programmes. To validate DNA-TF interactions in yeast, isolated plasmids encoding TFs were re-transformed into the yeast bait strain in which they were found to bind. To assess TF binding specificity, plasmids encoding TFs were also transformed into the yeast bait strains to which they do not bind.

### **Yeast cell spotting**

Yeast bait strains transformed with plasmids encoding TFs were grown overnight until log or mid-log phase at 30°C in liquid yeast CM medium supplemented with Histidine (CM +HIS -LEU). Cultures were normalized to an OD<sub>600</sub> of 0.4, spotted onto solid medium CM +HIS -LEU or CM -HIS -LEU + 3-AT, and grown for 3 days at 30°C.

### **Isolation and transformation of maize mesophyll protoplasts**

Maize mesophyll protoplasts were isolated from 10-day-old maize greening plants and transformed according to Lourenço et al. (2013) with minor modifications. Mid-section of newly matured second leaves was digested in a cell wall digestive medium containing 1.5% (w/v) cellulase R-10 (Duchefa), 0.3% (w/v) macerozyme R-10

(Duchefa), 10 mM MES (pH 5.7), 0.4 M mannitol, 1 mM CaCl<sub>2</sub>, 0.1% (w/v) BSA and 5 mM  $\beta$ -mercaptoethanol. Several leaf blades were stacked and cut perpendicularly to the long axis into 0.5 to 1 mm slices and quickly transferred to digestive medium (25 mL digestive medium for each set of 10 leaf blades). Purity and integrity of isolated protoplasts were examined under light microscopy. Mesophyll protoplasts were quantified and its abundance adjusted to  $2 \times 10^6$  protoplasts/mL. Transformed protoplasts were resuspended in 1.25 mL of incubation solution (0.6 M mannitol, 4 mM MES (pH 5.7) and 4 mM KCl) and incubated in 24-well plates for 18h at room temperature under dark.

### **Bimolecular Fluorescence Complementation (BiFC) assay**

To generate BiFC constructs, full-length coding sequences (CDS) of *ZmbHLH128* (GRMZM2G314882) and *ZmbHLH129* (GRMZM5G856837) were PCR-amplified using respectively the following pairs of *attB*-containing primers: 5'-GGGGACAAGTTTGTACAAAAAAGCAGGCTNNATGATGAACTGCGCCGGA-3' / 5'-GGGGACCACTTTGTACAAGAAAGCTGGGTNCTAAGCATTAGGCGGCCAG-3', and 5'-GGGGACAAGTTTGTACAAAAAAGCAGGCTNNATGATGGACTGCGCTGGA-3' / 5'-GGGGACCACTTTGTACAAGAAAGCTGGGTNCTAAGCATTTGGGGGCCAG-3' (underlined sequences indicate *attB* Gateway adaptors). *ZmbHLH128* and *ZmbHLH129* CDS were recombined into pDONR221 (Invitrogen) to obtain Entry clones through BP-Gateway reaction (Invitrogen), following the manufacturer's instructions. CDS were then recombined into vectors YFP<sup>N</sup>43 and YFP<sup>C</sup>43 through LR-Gateway reaction (Invitrogen) to raise a translational fusion with N- and C-terminal domains of yellow fluorescent protein (YFP), respectively. Final BiFC constructs were denominated as YFP<sup>N</sup>::*ZmbHLH128*, YFP<sup>N</sup>::*ZmbHLH129*, YFP<sup>C</sup>::*ZmbHLH128*, and YFP<sup>C</sup>::*ZmbHLH129*. Maize mesophyll protoplasts were transformed with 6  $\mu$ g of each of the BiFC constructs. Protoplasts transformed with YFP<sup>N</sup>::Akin10 (*Arabidopsis* SNF1 Kinase Homolog 10), YFP<sup>C</sup>::Akin3 (*Arabidopsis* SNF1 Kinase Homolog 3) and YFP<sup>N</sup>43 and YFP<sup>C</sup>43 empty vectors were used as negative controls. Transformations were performed in triplicate. YFP fluorescence and chlorophyll autofluorescence signals were observed under a confocal microscope (Leica SP5).

## Transient expression assays *in planta*

For the transient expression assays in tobacco leaves, reporter and effector constructs were generated in the Gateway binary vectors pGWB3i (pGWB3 containing an intron-tagged  $\beta$ -glucuronidase (GUS) open reading frame (Berger et al. 2007)) and pGWB2 (Tanaka et al. 2012), respectively.

To construct the reporter plasmids, promoter fragments of *ZmC<sub>4</sub>-NADP-ME* (GRMZM2G085019, from -389 to -154 bp) and *ZmnonC<sub>4</sub>-NADP-ME* (GRMZM2G122479, from -368 to -143 bp) were fused to a 136 bp minimal *CaMV35S* promoter (*m35S*) in a 3-step PCR reaction: (1) promoter sequences were amplified with long chimeric primers to introduce overlapping ends (reverse primer of *pZmC<sub>4</sub>-NADP-ME* / *pZmnonC<sub>4</sub>-NADP-ME* was designed to be complementary to the forward primer of the *m35S*) (supplementary table S4); (2) promoter sequences amplified by PCR in (1) were mixed according to the fusion products of interest in a ratio of 1:1 (*ZmC<sub>4</sub>-NADP-ME* (-389 to -154 bp)::*m35S* and *ZmnonC<sub>4</sub>-NADP-ME* (-368 to -143 bp)::*m35S*) and 10 PCR cycles were run without primers (denaturation at 98°C for 10 s, 55°C for 30 s, and 72°C for 1 min); and (3) fusion products of interest were amplified with *attB*-containing primers (supplementary table S4). To obtain Entry clones, promoter fragments fused to *m35S* were cloned into pDONR221 (Invitrogen) through BP-Gateway reaction (Invitrogen), following the manufacturer's instructions. Promoter sequences were then recombined into the binary vector pGWB3i through LR-Gateway reaction (Invitrogen) to obtain the final reporter constructs for *promoter::GUS* analysis (*pZmC<sub>4</sub>-NADP-ME* and *pZmnonC<sub>4</sub>-NADP-ME*). For the effector constructs (TF driven by the *CaMV35S* promoter), *ZmbHLH128* and *ZmbHLH129* Entry clones previously generated (see BiFC assay) were directly recombined into the binary vector pGWB2 through LR-Gateway reaction (Invitrogen). Reporter and effector constructs together with a construct harbouring the silencing suppressor P1b (Valli et al. 2006) were transformed into the *Agrobacterium tumefaciens* strain GV301. Overnight cultures of *Agrobacterium* harbouring reporter, effector and P1b constructs were sedimented (5000 g for 15 min, at 4°C) and resuspended in infiltration medium (10 mM MgCl<sub>2</sub>, 10 mM MES (pH 5.6), 200  $\mu$ M acetosyringone) to an OD<sub>600</sub> of 0.3, 1, and 0.5, respectively, and mixed in a ratio of 1:1:1. Mixed *Agrobacterium* cultures were incubated for 2h at 28°C and used to spot-



infiltrate the abaxial side of 5-week-old tobacco leaves. As controls, tobacco leaves were agro-infiltrated with mixed cultures carrying the reporter construct alone or the empty vector pGWB3i and effector constructs. Infected leaves were analysed at 96h post-infiltration. Leaf discs of 2.5 cm in diameter were collected from the infiltrated spots and used for the quantification of GUS activity. GUS activity was quantified by measuring the rate of 4-methylumbelliferyl- $\beta$ -D-glucuronide (MUG) conversion to 4-methylumbelliferone (MU) as described in Jefferson et al. (1987) and Williams et al. (2016). Briefly, soluble protein was extracted from agro-infiltrated tobacco leaf discs by freezing in liquid nitrogen and maceration, followed by addition of protein extraction buffer. Diluted protein extracts (1:2) were incubated with 1 mM MUG for 30, 60, 90 and 120 min at 37°C in a 96-well plate. GUS activity was terminated at the end of each time point by the addition of 200 mM Na<sub>2</sub>CO<sub>3</sub> and MU fluorescence measured by exciting at 365 nm and measuring emission at 455 nm. The concentration of MU/unit fluorescence in each sample was interpolated using a concentration gradient of MU from 1.5 to 800  $\mu$ M MU.

### **Production of recombinant ZmbHLH128 and ZmbHLH129**

*ZmbHLH128* and *ZmbHLH129* full-length CDS were PCR-amplified using, respectively, the following pairs of gene specific primers 5'-GAATTCATGATGAACTGCGCCGGA-3' / 5'-CTCGAGCTAAGCATTAGGCGGCCAG-3' and 5'-GAATTCATGATGGACTGCGCTGGA-3' / 5'-CTCGAGCTAAGCATTTGGGGGCCAG-3' (underlined sequences indicate adaptors with restriction enzyme sites). *ZmbHLH128* and *ZmbHLH129* were cloned as *EcoRI*-*XhoI* fragments into the expression vector pET32a (Novagen), generating N-terminal Trx-tagged fusions. pET32a-Trx::*ZmbHLH128* and pET32a-Trx::*ZmbHLH129* constructs were confirmed by sequencing and transformed into Rosetta (DE3)pLysS competent cells (Invitrogen) for protein expression. Cells transformed with pET32a-Trx::*ZmbHLH128* and pET32a-Trx::*ZmbHLH129* constructs were respectively grown in Terrific Broth (TB) and Luria-Bertani (LB) medium to an OD<sub>600</sub> of 0.5. Protein expression was induced with 4 mM isopropyl-d-1-thiogalactopyranoside (IPTG) and allowed to occur for 3h (*ZmbHLH128*) or 5h (*ZmbHLH129*) at 30°C. Protein purification was performed as described in Cordeiro et al. (2016).

## **Blue Native-Polyacrylamide gel electrophoresis (BN-PAGE) and western blotting**

Molecular mass of oligomers co-existing in purified ZmbHLH128 and ZmbHLH129 recombinant proteins was determined by blue native polyacrylamide gel electrophoresis (BN-PAGE). Two micrograms of the recombinant proteins (Trx::His::ZmbHLH128 or Trx::His::ZmbHLH129) were resolved on a 3-12% Novex Bis-Tris NativePAGE mini gel (Life Technologies), following the manufacturer's instructions. HMW Native Marker Kit (66 - 669 kDa, GE Healthcare) was used to estimate molecular mass. Resolved proteins were transferred to a polyvinylidene difluoride (PVDF) membrane (GE Healthcare). The membrane was destained with a 50% (v/v) methanol and 10% (v/v) acid acetic solution followed by pure methanol. For immunodetection of Trx::His::ZmbHLH128 and Trx::His::ZmbHLH129, the membrane was incubated with  $\alpha$ -His antibody (GE Healthcare) followed by  $\alpha$ -mouse horseradish peroxidase-conjugated antibody (abcam) for 1h each at room temperature.

## **Electrophoretic Mobility Shift Assay (EMSA)**

DNA probes were generated by annealing oligonucleotide pairs in a thermocycler followed by radiolabeling as described in Serra et al. (2013). DNA probe sequences and respective annealing temperatures are listed in supplementary table S3. EMSAs were performed using 400 ng of the recombinant proteins Trx::ZmbHLH128 or Trx::ZmbHLH129, and 50 fmol of radiolabeled probes. Competition assays were performed adding 200- to 400-fold molar excess of the unlabeled probe. Trx::OsPIF14 (LOC\_Os07g05010) and Trx protein, both purified by Cordeiro et al. (2016), were used as negative controls. Each protein was mixed with probes in a 10  $\mu$ l reaction containing 10 mM HEPES (pH 7.9), 40 mM KCl, 1 mM EDTA (pH 8), 1 mM DTT, 50 ng herring sperm DNA, 15  $\mu$ g BSA and 10% (v/v) glycerol. Binding reactions were incubated for 1h on ice and the bound complexes resolved on a native 5% polyacrylamide gel (37.5:1). Gel electrophoresis and detection of radioactive signal were performed as described in Serra et al. (2013).

## **Synten analysis**

SynFind (Tang et al. 2015) was used to identify maize syntenic chromosomal regions for *ZmbHLH128* (GRMZM2G314882) and *ZmbHLH129* (GRMZM5G856837) genes against *Z. mays* B73 RefGen\_v3 genome. A table containing maize syntelog gene pairs was retrieved using SynFind tool (supplementary table S2).

### Phylogenetic analyses

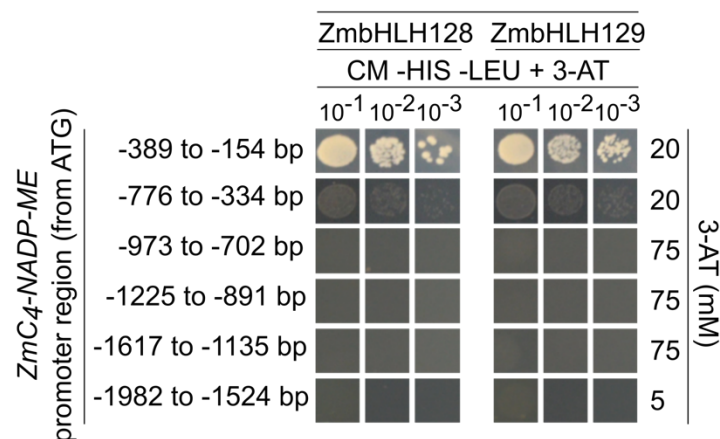
*ZmbHLH128* and *ZmbHLH129* were used as references to identify closely related *bHLH* genes of *Zea mays*, *Sorghum bicolor*, *Setaria viridis*, *Setaria italica*, *Oryza sativa*, and *Brachypodium distachyon*, through Phytozome database (Goodstein et al. 2012). Predicted CDS were aligned using MUSCLE. The resulting alignment was used to infer a maximum likelihood phylogenetic tree, using GTR+G+I nucleotide substitution model (1000 bootstrap pseudoreplicates) in MEGA 7 software (Kumar et al. 2016). Phylogenetic analysis of genes encoding C<sub>3</sub> and C<sub>4</sub> plastidic NADP-ME isoforms from *B. distachyon* (BRADI2g05620), *O. sativa* (LOC\_Os01g09320), *D. oligosanthos* (Do024386), *S. italica* (Si000645), *S. bicolor* (Sobic.003g036200, Sobic.009G108700) and *Z. mays* (GRMZM2G085019, GRMZM2G122479) was performed using Geneious Pro 5.3.6 software (Kearse et al. 2012). Full-length genomic sequences were aligned using MUSCLE. Phylogenetic tree was inferred using the Neighbor Joining (1000 bootstrap pseudoreplicates) and rooted using the gene encoding C<sub>3</sub> plastidic NADP-ME (At1g79750) from *Arabidopsis thaliana*, a dicot angiosperm.

701 **Figures**702 **FIG. 1.**

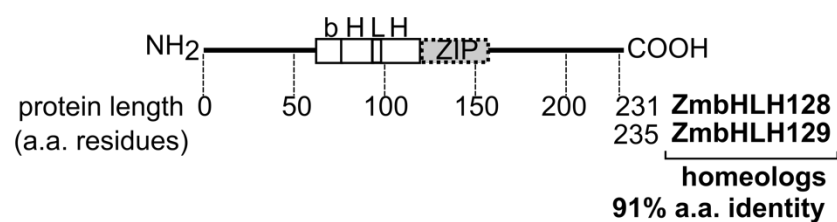
A



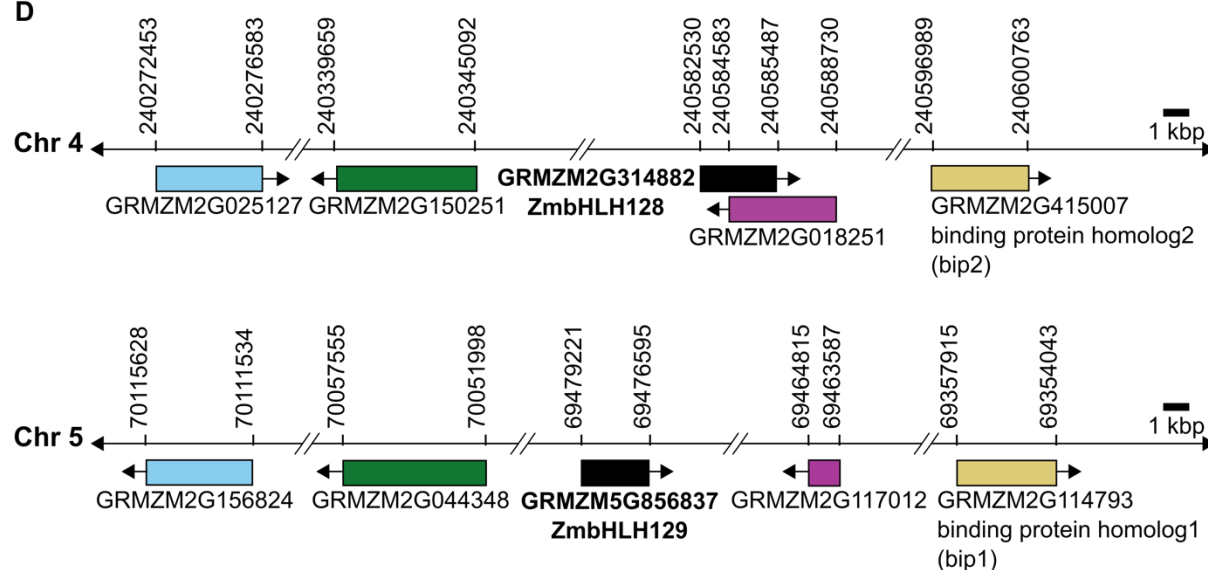
B



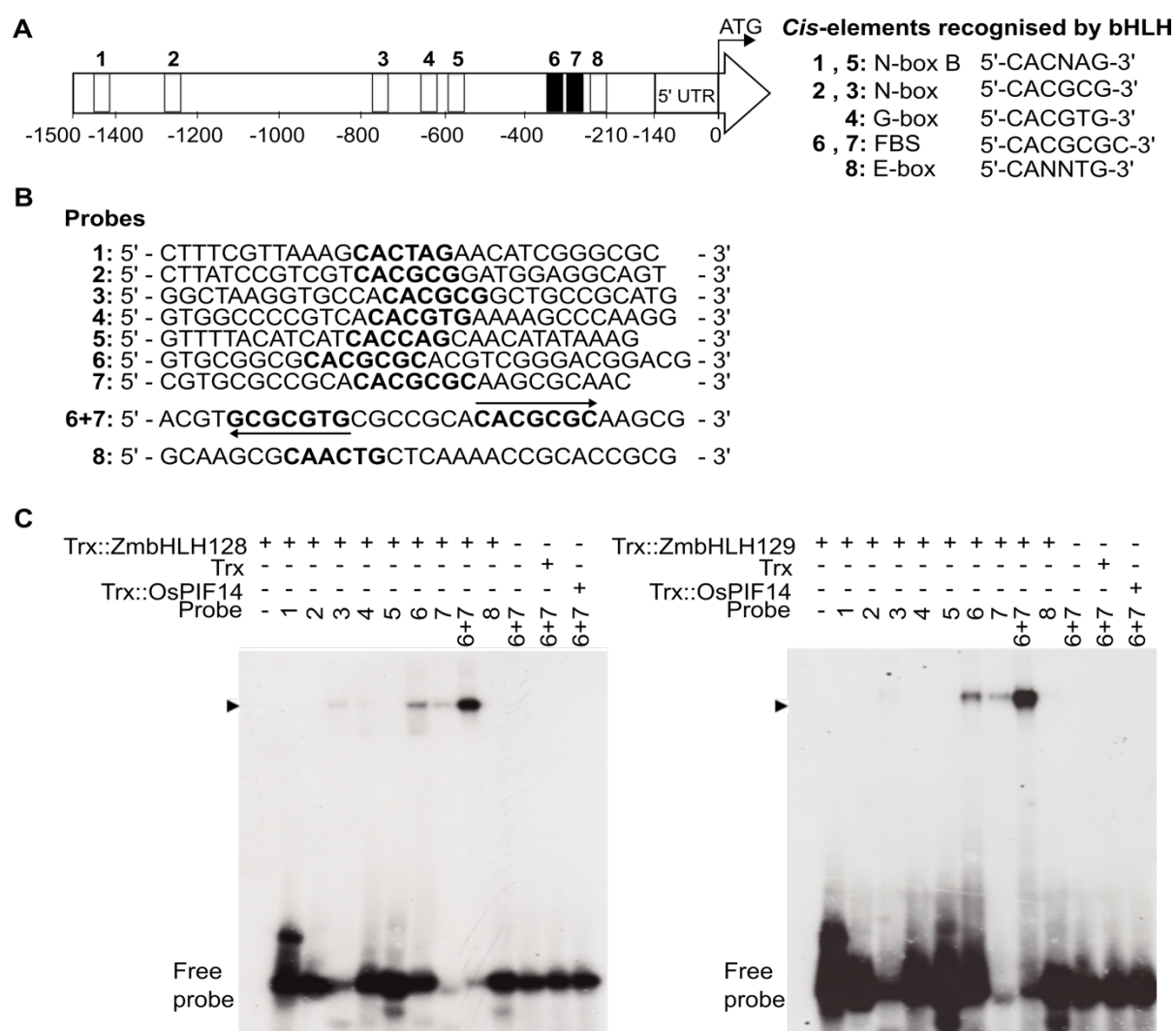
C

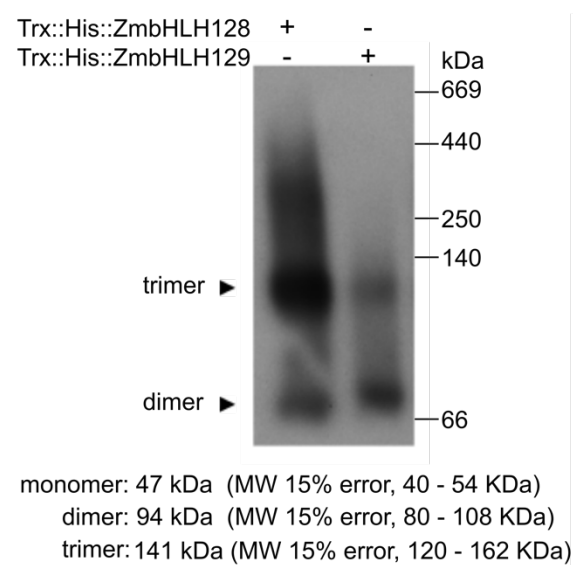
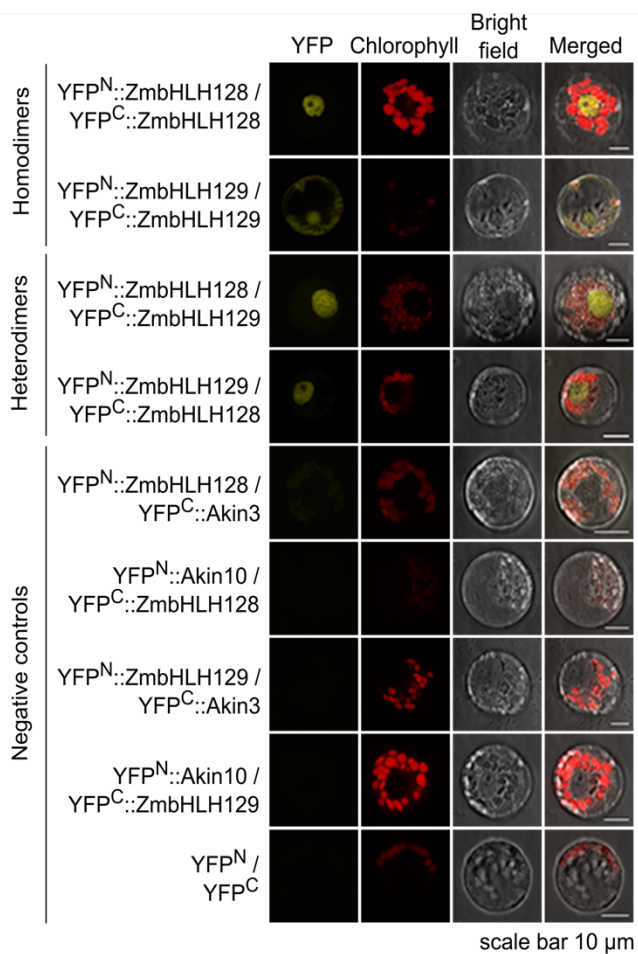


D

703  
704

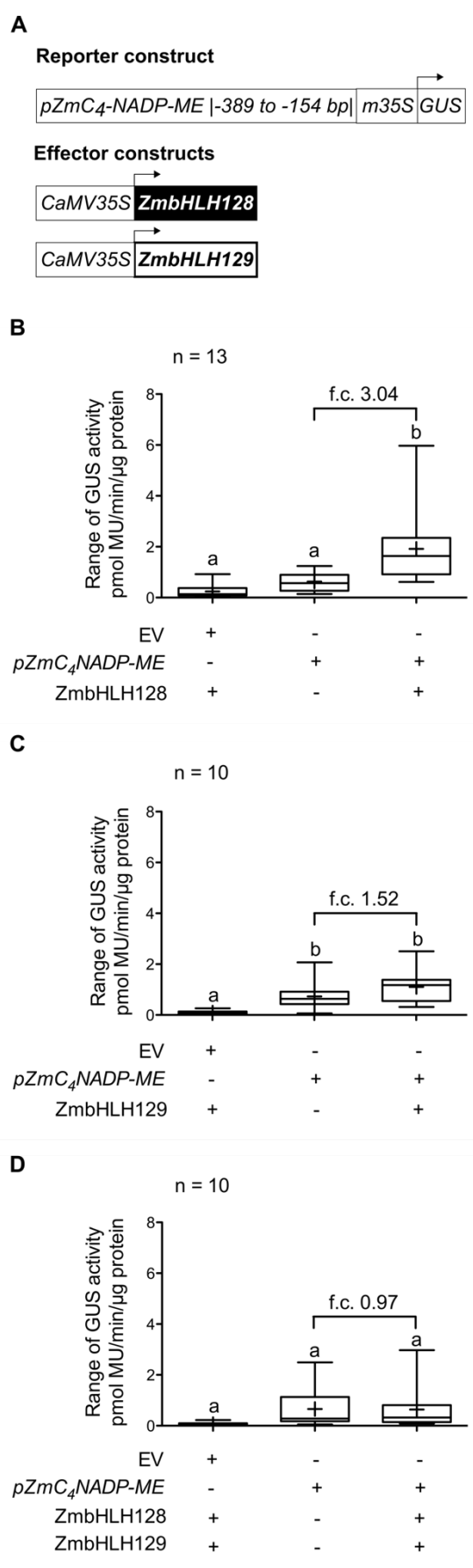
**FIG. 2.**



**FIG. 3.****A****B**

711 **FIG. 4.**

712

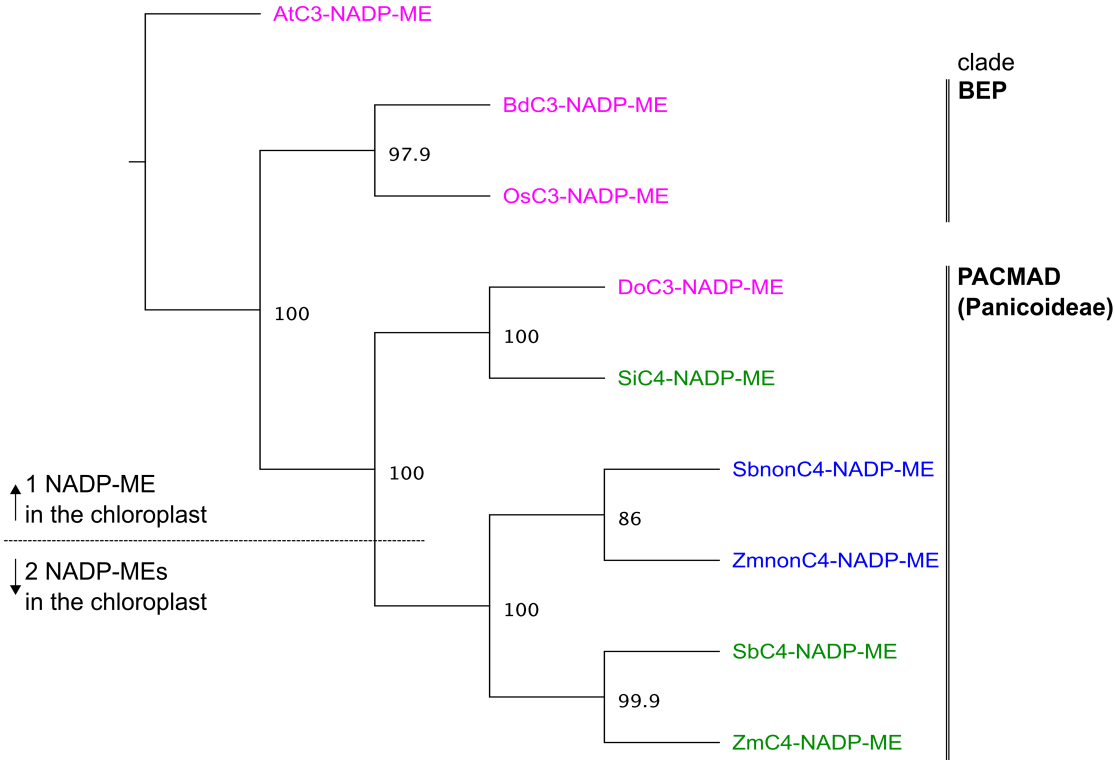




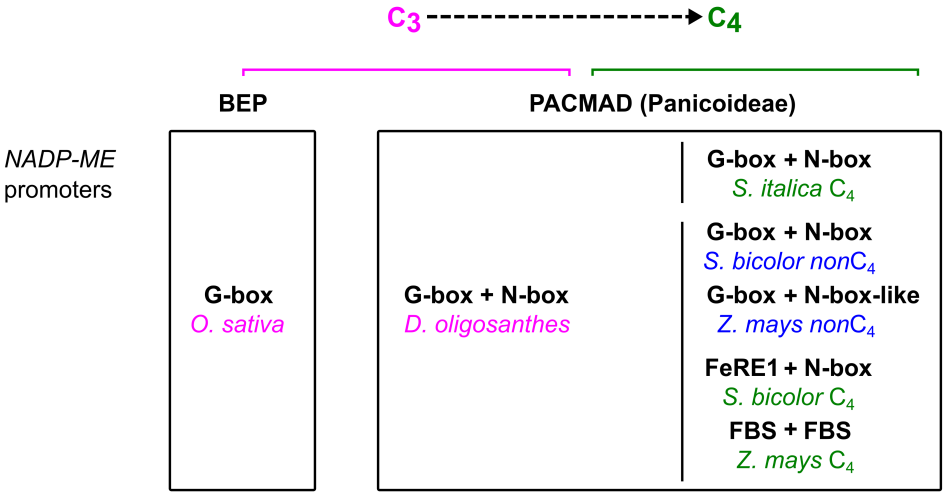


716 **FIG. 6.**

A



B



717  
718

## Figure legends

**FIG. 1.** ZmbHLH128 and ZmbHLH129 homeologs bind the *ZmC<sub>4</sub>-NADP-ME* promoter. (A) Schematic representation of the *ZmC<sub>4</sub>-NADP-ME* promoter, divided into fragments used as baits in Y1H screenings, and the ZmbHLH TFs identified. ATG and TAG are the translational start codon and the stop codon of the *ZmC<sub>4</sub>-NADP-ME* ORF, respectively. ZmbHLH position on the scheme indicates that they bind between the base pairs -389 and -154 in relation to the ATG. (B) Analysis of ZmbHLH-*pZmC<sub>4</sub>-NADP-ME* binding specificity. Each of the six yeast bait strains was transformed with both ZmbHLHs (pAD-GAL4-2.1::TF vectors) and positive interactions selected on CM -HIS -LEU + 3-AT (yeast Complete Minimal medium lacking histidine and leucine amino acids, and supplemented with 3-amino-1,2,4-triazole (3-AT), a competitive inhibitor of the *HIS3* gene product). (C) Schematic representation of basic Helix-Loop-Helix (bHLH) and leucine zipper (ZIP) protein domains, and respective position in protein sequences. (D) Schematic representation of *ZmbHLH128* and *ZmbHLH129* (black) and four additional maize homeolog gene pairs located in syntenic regions of chromosomes 4 and 5. Homeolog genes are indicated by colour. Arrows indicate direction of transcription of each gene. Genomic coordinates provided from the B73 RefGen\_v3 assembly version.

**FIG. 2.** ZmbHLH128 and ZmbHLH129 bind two FBS *cis*-elements present in *ZmC<sub>4</sub>-NADP-ME* promoter. (A) Schematic representation of position and nucleotide sequence of eight *cis*-elements recognised by bHLH that were identified in the *ZmC<sub>4</sub>-NADP-ME* promoter. FBS stands for FHY3/FAR1 Binding Site and it is a N-box-containing motif. (B) EMSA probe sequences used to test *in vitro* binding affinity of ZmbHLH128 and ZmbHLH129 to *cis*-elements (highlighted in bold). Arrows indicate that the FBS *cis*-elements are present in opposite orientations. (C) EMSAs showing *in vitro* binding affinity of Trx::ZmbHLH128 (gel on the left) and Trx::ZmbHLH129 (gel on the right) to the radiolabeled probes described in (B). Arrowheads indicate uplifted ZmbHLH-DNA probe complexes. Free probe indicates unbound DNA probes.

**FIG. 3.** ZmbHLH128 and ZmbHLH129 form both homo- and heterodimers. (A) Western blot of BN-PAGE for the recombinant proteins Trx::His::ZmbHLH128 and

Trx::His::ZmbHLH129. Gel was loaded with equivalent amount of protein. Recombinant proteins were immunodetected using  $\alpha$ -His antibody. MW indicates molecular-weight size marker. (B) Protein interactions between ZmbHLH128 and ZmbHLH129 were tested by BiFC in maize mesophyll protoplasts co-transformed with constructs expressing ZmbHLH128 and ZmbHLH129 fused to N- and C-terminal YFP domains. YFP<sup>N</sup> and YFP<sup>C</sup> indicate split N- and C-terminal YFP domains, respectively.

**FIG. 4.** ZmbHLH129 impairs *trans*-activation of the *ZmC<sub>4</sub>-NADP-ME* promoter by ZmbHLH128. (A) Schematic representation of reporter and effector constructs used in transient expression assays in leaves of *Nicotiana benthamiana*. Reporter construct contains *GUS* gene driven by the minimal *CaMV35S* promoter (m35S) fused to *pZmC<sub>4</sub>-NADP-ME* (-389 to -154 bp). Effector constructs contain the *ZmbHLH128* or *ZmbHLH129* CDS driven by the full *CaMV35S* promoter. (B-D) Box plots (2.5 to 97.5 percentiles) showing *GUS* activity, expressed in picomoles of the reaction product 4-methylumbelliferone (MU) generated per minute per microgram of protein, in leaves agro-infiltrated with reporter and the following effector constructs: (B) *ZmbHLH128*, (C) *ZmbHLH129*, and (D) *ZmbHLH128* and *ZmbHLH129*. Different letters denote differences in experimental data that are statistically significant (One-way ANOVA, Tukey test,  $p \leq 0.05$ ,  $n = 10-13$ ). EV indicates pGWB3i empty vector (no promoter fragment cloned). Cross inside box plots indicates mean. f.c. indicates fold-change.

**FIG. 5.** The G-box-based *cis*-element pair recognised by ZmbHLH128 and ZmbHLH129 in *NADP-ME* promoters operates synergistically. (A) Sequence alignment of the two FBS *cis*-elements present in *ZmC<sub>4</sub>-NADP-ME* promoter against homologous *cis*-elements present in other promoters of genes encoding plastidic *NADP-ME*. C<sub>4</sub> grasses: *Zea mays*, *Sorghum bicolor* and *Setaria italica*; C<sub>3</sub> grasses: *Dichanthelium oligosanthes*, *Oryza sativa* and *Brachypodium distachyon*. Plastidic *NADP-MEs* are colour-coded: green for C<sub>4</sub>, blue for *nonC<sub>4</sub>* and magenta for C<sub>3</sub>. *Cis*-elements are highlighted in bold and coloured according to the *NADP-ME* they belong to. FBS stands for FHY3/FAR1 Binding Site and FeRE1 for Iron Responsive Element 1. (B) EMSA probes used to test *in vitro* binding affinity of ZmbHLH128 and

ZmbHLH129 to each *cis*-element described in (A). Probe sequences are listed in supplementary table S3. (C) EMSA assays showing *in vitro* binding affinity of Trx::ZmbHLH128 (gel on the left) and Trx::ZmbHLH129 (gel on the right) proteins to the probes described in (B). Arrowheads indicate uplifted ZmbHLH-DNA probe complexes. Free probe indicates unbound DNA probes.

**FIG. 6.** Acquisition of N-box-derived *cis*-elements in *NADP-ME* promoters facilitates ZmbHLH128 and ZmbHLH129 binding in PACMAD Panicoid grasses. (A) Phylogenetic tree of genes encoding plastidic NADP-ME from C<sub>3</sub> and C<sub>4</sub> grass species. C<sub>3</sub>: *Brachypodium distachyon* (Bd), *Oryza sativa* (Os) and *Dichanthelium oligosanthes* (Do); C<sub>4</sub>: *Setaria italica* (Si), *Sorghum bicolor* (Sb) and *Zea mays* (Zm). *NADP-MEs* are colour-coded: magenta for C<sub>3</sub>, blue for *non*C<sub>4</sub> and green for C<sub>4</sub>. *NADP-ME* genomic sequences were aligned using MUSCLE, and the phylogenetic tree inferred by NJ method (1000 bootstrap pseudoreplicates, node numbers indicate bootstrap values). Gene encoding C<sub>3</sub> plastidic NADP-ME from *Arabidopsis thaliana* (AtC<sub>3</sub>-NADP-ME) was used as outgroup. (B) Diagram representing C<sub>3</sub> to C<sub>4</sub> molecular evolution of homologous bHLH binding *cis*-elements identified in promoters of genes encoding plastidic NADP-ME. Dashed arrow indicates intermediate evolutionary steps from C<sub>3</sub> to C<sub>4</sub>. Vertical lines indicate two independent C<sub>4</sub> origins of *S. italica* and *S. bicolor* / *Z. mays* (Paniceae and Andropogoneae tribes, respectively).

## Acknowledgments

We thank Lisete Fernandes (Escola Superior de Tecnologia da Saúde de Lisboa, Portugal) for discussions and advice concerning EMSA experiments, Cecília Arraiano Lab (ITQB-NOVA, Oeiras, Portugal) for material used in EMSA experiments, Myriam Goudet and Samuel Brockington (Department of Plant Sciences, University of Cambridge, UK) for assistance with phylogenetic analyses. This work was supported by European Union project *3to4* (Grant agreement no: 289582) and Fundação para a Ciência e Tecnologia (FCT) through research unit GREEN-it 'Bioresources for Sustainability' (UID/Multi/04551/2013). ARB (SFRH/BD/105739/2014), AG (SFRH/BD/89743/2012), AMC (SFRH/BD/74946/2010), PMB (SFRH/BPD/86742/2012), IAA (IF/00960/2013 – POPH-QREN), and NJMS (IF/01126/2012 – POPH-QREN) were funded by FCT, TSS and PG by European Union project *3to4* (Grant agreement no: 289582), and IR-L by BBSRC grant (BB/L014130).

## References

- Agrawal NJ, Radhakrishnan R, Purohit PK. 2008. Geometry of mediating protein affects the probability of loop formation in DNA. *Biophys. J.* 94:3150–3158.
- Alvarez CE, Saigo M, Margarit E, Andreo CS, Drincovich MF. 2013. Kinetics and functional diversity among the five members of the NADP-malic enzyme family from *Zea mays*, a C<sub>4</sub> species. *Photosynth. Res.* 115:65–80.
- Atchley WR, Terhalle W, Dress A. 1999. Positional dependence, cliques, and predictive motifs in the bHLH protein domain. *J. Mol. Evol.* 48:501–5016.
- Berger B, Stracke R, Yatusovich R, Weisshaar B, Flügge UI, Gigolashvili T. 2007. A simplified method for the analysis of transcription factor-promoter interactions that allows high-throughput data generation. *Plant J.* 50:911–916.
- Bowes G, Ogren WL, Hageman RH. 1971. Phosphoglycolate production catalyzed by ribulose diphosphate carboxylase. *Biochem. Biophys. Res. Commun.* 45:716–722.
- Brown NJ, Newell CA, Stanley S, Chen JE, Perrin AJ, Kajala K, Hibberd JM. 2011. Independent and parallel recruitment of preexisting mechanisms underlying C<sub>4</sub> photosynthesis. *Science* 331:1436–1439.
- Calvin BM, Massini P. 1952. The path of carbon in photosynthesis. *Experientia* VIII:445–457.
- Christin P-A, Besnard G, Samaritani E, Duvall MR, Hodkinson TR, Savolainen V. 2008. Report oligocene CO<sub>2</sub> decline promoted C<sub>4</sub> photosynthesis in grasses. *Curr. Biol.* 18:37–43.
- Christin P-A, Boxall SF, Gregory R, Edwards EJ, Hartwell J, Osborne CP. 2013. Parallel recruitment of multiple genes into C<sub>4</sub> photosynthesis. *Genome Biol. Evol.* 5:2174–2187.
- Christin P-A, Osborne CP. 2014. The evolutionary ecology of C<sub>4</sub> plants. *New Phytol.* 204:765–781.
- Christin P-A, Osborne CP, Sage RF, Edwards EJ. 2011. C<sub>4</sub> eudicots are not younger than C<sub>4</sub> monocots. *J. Exp. Bot.* 62:3171–3181.
- Christin P-A, Salamin N, Kellog EA, Vincentini A, Besnard G. 2009. Integrating phylogeny into studies of C<sub>4</sub> variation in the grasses. *New Phytol.* 149:82–87.
- Cordeiro AM, Figueiredo DD, Tepperman J, Borba AR, Lourenço T, Abreu IA, Ouwerkerk PBF, Quail PH, Margarida Oliveira M, Saibo NJM. 2016. Rice phytochrome-interacting factor protein OsPIF14 represses *OsDREB1B* gene

- expression through an extended N-box and interacts preferentially with the active form of phytochrome B. *Biochim. Biophys. Acta* 1859:393–404.
- De Masi F, Grove CA, Vedenko A, Alibés A, Gisselbrecht SS, Serrano L, Bulyk ML, Walhout AJM. 2011. Using a structural and logics systems approach to infer bHLH-DNA binding specificity determinants. *Nucleic Acids Res.* 39:4553–4563.
- Ehleringer JR, Monson RK. 1993. Evolutionary and ecological aspects of photosynthetic pathway variation. *Annu. Rev. Ecol. Evol. Syst.* 24:411–439.
- Emms DM, Covshoff S, Hibberd JM, Kelly S. 2016. Independent and parallel evolution of new genes by gene duplication in two origins of C<sub>4</sub> photosynthesis provides new insight into the mechanism of phloem loading in C<sub>4</sub> species. *Mol. Biol. Evol.* 33:1796–1806.
- Fisher A, Caudy M. 1998. The function of hairy-related bHLH repressor proteins in cell fate decisions. *BioEssays* 20:298–306.
- Goodstein DM, Shu S, Howson R, Neupane R, Hayes RD, Fazo J, Mitros T, Dirks W, Hellsten U, Putnam N, Rokhsar DS. 2012. Phytozome: a comparative platform for green plant genomics. *Nucleic Acids Res.* 40:D1178–D1186.
- Gordân R, Shen N, Dror I, Zhou T, Horton J, Rohs R, Bulyk ML. 2013. Genomic regions flanking E-box binding sites influence DNA binding specificity of bHLH transcription factors through DNA shape. *Cell Rep.* 3:1093–1104.
- Gowik U, Burscheidt J, Akyildiz M, Schlue U, Koczor M, Streubel M, Westhoff P. 2004. Cis-regulatory elements for mesophyll-specific gene expression in the C<sub>4</sub> plant *Flaveria trinervia*, the promoter of the C<sub>4</sub> phosphoenolpyruvate carboxylase gene. *Plant Cell* 16:1077–1090.
- Gowik U, Schulze S, Saladié M, Rolland V, Tanz SK, Westhoff P, Ludwig M. 2016. A MEM1-like motif directs mesophyll cell-specific expression of the gene encoding the C<sub>4</sub> carbonic anhydrase in *Flaveria*. *J. Exp. Bot.* 68:311–320.
- Grass Phylogeny Working Group II. 2012. New grass phylogeny resolves deep evolutionary relationships and discovers C<sub>4</sub> origins. *New Phytol.* 193:304–312.
- Grove CA, Masi F, Barrasa MI, Newburger DE, Alkema MJ, Bulyk ML, Walhout AJM. 2009. A multiparameter network reveals extensive divergence between *C. elegans* bHLH transcription factors. *Cell* 138:314–327.
- Haberlandt GFJ. 1904. Physiologische Pflanzenanatomie. Leipzig W. Engelmann.
- Hatch MD. 1987. C<sub>4</sub> photosynthesis: a unique blend of modified biochemistry, anatomy and ultrastructure. *Biochim. Biophys. Acta* 895:81–106.

- 889 Hatch MD, Slack CR. 1966. Photosynthesis by sugar-cane leaves. A new  
 890 carboxylation reaction and the pathway of sugar formation. *Biochem. J.*  
 891 101:103–111.
- 892 Hibberd JM, Covshoff S. 2010. The regulation of gene expression required for C<sub>4</sub>  
 893 photosynthesis. *Annu. Rev. Plant Biol.* 61:181–207.
- 894 Huang P, Brutnell TP. 2016. A synthesis of transcriptomic surveys to dissect the  
 895 genetic basis of C<sub>4</sub> photosynthesis. *Curr. Opin. Plant Biol.* 31:91–99.
- 896 Jefferson RA, Kavanagh TA, Bevan MW. 1987. GUS fusions:  $\beta$ -glucuronidase as a  
 897 sensitive and versatile gene fusion marker in higher plants. *EMBO J.* 6:3901–  
 898 3907.
- 899 Kagawa T, Hatch MD. 1974. C<sub>4</sub>-acids as the source of carbon dioxide for Calvin  
 900 cycle photosynthesis by bundle sheath cells of the C<sub>4</sub>-pathway species *Atriplex*  
 901 *spongiosa*. *Biochem. Biophys. Res. Commun.* 59:1326–1332.
- 902 Kajala K, Brown NJ, Williams BP, Borrill P, Taylor LE, Hibberd JM. 2012. Multiple  
 903 Arabidopsis genes primed for recruitment into C<sub>4</sub> photosynthesis. *Plant J.*  
 904 69:47–56.
- 905 Kang SG, Price J, Lin PC, Hong JC, Jang JC. 2010. The Arabidopsis bZIP1  
 906 transcription factor is involved in sugar signaling, protein networking, and DNA  
 907 binding. *Mol. Plant* 3:361–373.
- 908 Kearse M, Moir R, Wilson A, Stones-Havas S, Cheung M, Sturrock S, Buxton S,  
 909 Cooper A, Markowitz S, Duran C, et al. 2012. Geneious Basic: an integrated  
 910 and extendable desktop software platform for the organization and analysis of  
 911 sequence data. *Bioinformatics* 28:1647–1649.
- 912 Kim JJ, Kang H, Park J, Kim W, Yoo J, Lee N, Kim JJ, Yoon T, Choi G. 2016. PIF1-  
 913 interacting transcription factors and their binding sequence elements determine  
 914 the *in vivo* targeting sites of PIF1. *Plant Cell* 28:1388–1405.
- 915 Ku MSB, Agarie S, Nomura M, Fukayama H, Tsuchida H, Ono K, Hirose S, Toki S,  
 916 Miyao M, Matsuoka M. 1999. High-level expression of maize phosphoenol/  
 917 pyruvate carboxylase in transgenic rice plants. *Nat. Biotechnol.* 17:76–80.
- 918 Kumar S, Stecher G, Tamura K. 2016. MEGA7: Molecular Evolutionary Genetics  
 919 Analysis Version 7.0 for bigger datasets. *Mol. Biol. Evol.* 33:1870–1874.
- 920 Langdale JA. 2011. C<sub>4</sub> cycles: past, present, and future research on C<sub>4</sub>  
 921 photosynthesis. *Plant Cell* 23:3879–3892.



- 922 Li G, Siddiqui H, Teng Y, Lin R, Wan X, Li J, Lau O-S, Ouyang X, Dai M, Wan J, et  
 923 al. 2011. Coordinated transcriptional regulation underlying the circadian clock in  
 924 *Arabidopsis*. *Nat. Cell Biol.* 13:616–622.
- 925 Li X, Duan X, Jiang H, Sun Y, Tang Y, Yuan Z, Guo J. 2006. Genome-wide analysis  
 926 of basic/helix-loop-helix transcription factor family in rice and *Arabidopsis*. *Plant*  
 927 *Physiol.* 141:1167–1184.
- 928 Lin R, Ding L, Casola C, Ripoll DR, Feschotte C, Wang H. 2007. Transposase-  
 929 derived transcription factors regulate light signaling in *Arabidopsis*. *Science*  
 930 318:1302–1305.
- 931 Lloyd J, Farquhar GD. 1994.  $^{13}\text{C}$  discrimination during  $\text{CO}_2$  assimilation by the  
 932 terrestrial biosphere. *Oecologia* 99:201–215.
- 933 Lourenço T, Sapeta H, Figueiredo DD, Rodrigues M, Cordeiro A, Abreu IA, Saibo  
 934 NJM, Oliveira MM. 2013. Isolation and characterization of rice (*Oryza sativa* L.)  
 935 E3-ubiquitin ligase *Oshos1* gene in the modulation of cold stress response.  
 936 *Plant Mol. Biol.* 83:351–363.
- 937 Lundgren MR, Christin P-A. 2016. Despite phylogenetic effects,  $\text{C}_3$ – $\text{C}_4$  lineages  
 938 bridge the ecological gap to  $\text{C}_4$  photosynthesis. *J. Exp. Bot.* 68:241–254.
- 939 Maier A, Zell MB, Maurino VG. 2011. Malate decarboxylases: evolution and roles of  
 940 NAD(P)-ME isoforms in species performing  $\text{C}_4$  and  $\text{C}_3$  photosynthesis. *J. Exp.*  
 941 *Bot.* 62:3061–3069.
- 942 Martínez-García JF, Huq E, Quail PH. 2000. Direct targeting of light signals to a  
 943 promoter element-bound transcription factor. *Science* 288:859–863.
- 944 Massari ME, Murre C. 2000. Helix-loop-helix proteins: regulators of transcription in  
 945 eucaryotic organisms. *Mol. Cell. Biol.* 20:429–440.
- 946 Matsuoka M, Kyoizuka J, Shimamoto K, Kano-Murakami Y. 1994. The promoters of  
 947 two carboxylases in a  $\text{C}_4$  plant (maize) direct cell-specific, light-regulated  
 948 expression in a  $\text{C}_3$  plant (rice). *Plant J.* 6:311–319.
- 949 Maurino VG, Drincovich MF, Casati P, Andreo CS, Edwards GE, Ku MSB, Gupta  
 950 SK, Franceschi V. 1997. NADP-malic enzyme: immunolocalization in different  
 951 tissues of the  $\text{C}_4$  plant maize and the  $\text{C}_3$  plant wheat. *J. Exp. Bot.* 48:799–811.
- 952 Melzer R, Verelst W. 2009. The class E floral homeotic protein SEPALLATA3 is  
 953 sufficient to loop DNA in “floral quartet”-like complexes *in vitro*. *Nucleic Acids*  
 954 *Res.* 37:144–157.
- 955 Murre C, McCaw PS, Baltimore D. 1989. A new DNA binding and dimerization motif

- 956 in immunoglobulin enhancer binding, daughterless, MyoD, and myc proteins. *Cell*  
 957 56:777–783.
- 958 Nomura M, Sentoku N, Nishimura A, Lin J, Honda C, Taniguchi M, Ishida Y, Ohta S,  
 959 Komari T, Miyao-Tokutomi M, et al. 2000. The evolution of C<sub>4</sub> plants: acquisition  
 960 of *cis*-regulatory sequences in the promoter of C<sub>4</sub>-type pyruvate, orthophosphate  
 961 dikinase gene. *Plant J.* 22:211–221.
- 962 Ohsako S, Hyer J, Panganiban G, Oliver I, Caudy M. 1994. Hairy function as a DNA-  
 963 binding helix-loop-helix repressor of *Drosophila* sensory organ formation. *Genes*  
 964 *Dev.* 8:2743–2755.
- 965 Osborne CP, Beerling DJ. 2006. Nature's green revolution: the remarkable  
 966 evolutionary rise of C<sub>4</sub> plants. *Phil. Trans. R. Soc. B.* 361:173–194.
- 967 Ouwerkerk PB, Meijer AH. 2001. Yeast one-hybrid screening for DNA-protein  
 968 interactions. In: DNA-Protein Interactions. *Current Protocols in Molecular*  
 969 *Biology.* p. 12.12.1-12.12.22.
- 970 Patel M, Siegel AJ, Berry JO. 2006. Untranslated regions of *FbRbcS1* mRNA  
 971 mediate bundle sheath cell-specific gene expression in leaves of a C<sub>4</sub> plant. *J.*  
 972 *Biol. Chem.* 281:25485–25491.
- 973 Penfield S, Rylott EL, Gilday AD, Graham S, Larson TR, Graham IA. 2004. Reserve  
 974 mobilization in the Arabidopsis endosperm fuels hypocotyl elongation in the  
 975 dark, is independent of abscisic acid, and requires *PHOSPHOENOLPYRUVATE*  
 976 *CARBOXYKINASE1*. *Plant Cell* 16:2705–2718.
- 977 Rao X, Dixon RA. 2016. The differences between NAD-ME and NADP-ME subtypes  
 978 of C<sub>4</sub> photosynthesis: more than decarboxylating enzymes. *Front. Plant Sci.*  
 979 7:1525.
- 980 Reyna-Llorens I, Hibberd JM. 2017. Recruitment of pre-existing networks during the  
 981 evolution of C<sub>4</sub> photosynthesis. *Phil. Trans. R. Soc. B.* 372:20160386.
- 982 Rohs R, West SM, Sosinsky A, Liu P, Mann RS, Honig B. 2009. The role of DNA  
 983 shape in protein-DNA recognition. *Nature* 29:1248–1253.
- 984 Sage RF. 2004. The evolution of C<sub>4</sub> photosynthesis. *New Phytol.* 161:341–370.
- 985 Sage RF. 2016. A portrait of the C<sub>4</sub> photosynthetic family on the 50<sup>th</sup> anniversary of  
 986 its discovery: species number, evolutionary lineages, and hall of fame. *J. Exp.*  
 987 *Bot.* 67:4039–4056.
- 988 Sage RF, Christin P-A, Edwards EJ. 2011. The C<sub>4</sub> plant lineages of planet Earth. *J.*  
 989 *Exp. Bot.* 62:3155–3169.

- 990 Sasai Y, Kageyama R, Tagawa Y, Shigemoto R, Nakanishi S. 1992. Two  
 991 mammalian helix-loop-helix factors structurally related to *Drosophila hairy* and  
 992 *Enhancer of split*. *Genes Dev.* 6:2620–2634.
- 993 Serra TS, Figueiredo DD, Cordeiro AM, Almeida DM, Lourenço T, Abreu IA,  
 994 Sebastián A, Fernandes L, Contreras-Moreira B, Oliveira MM, et al. 2013.  
 995 OsRMC, a negative regulator of salt stress response in rice, is regulated by two  
 996 AP2/ERF transcription factors. *Plant Mol. Biol.* 82:439–455.
- 997 Sharkey TD. 1988. Estimating the rate of photorespiration in leaves. *Physiol. Plant.*  
 998 73:147–152.
- 999 Smaczniak C, Immink RG, Muiño JM, Blanvillain R, Busscher M, Busscher-Lange J,  
 1000 Dinh QD, Liu S, Westphal AH, Boeren S, et al. 2012. Characterization of MADS-  
 1001 domain transcription factor complexes in *Arabidopsis* flower development. *Proc.*  
 1002 *Natl. Acad. Sci. U. S. A.* 109:1560–1565.
- 1003 Smaczniak C, Muiño JM, Chen D, Angenent GC. 2017. Differences in DNA-binding  
 1004 specificity of floral homeotic protein complexes predict organ-specific target  
 1005 genes. *Plant Cell* doi:10.1105/tpc.17.00145.
- 1006 Tanaka Y, Kimura T, Hikino K, Goto S, Nishimura M, Mano S, Nakagawa T. 2012.  
 1007 Gateway vectors for plant genetic engineering: overview of plant vectors,  
 1008 application for bimolecular fluorescence complementation (BiFC) and multigene  
 1009 construction. In: Barrera-Saldaña HA, editor. *Genetic Engineering - Basics, New*  
 1010 *Applications and Responsibilities*. p. 35–58.
- 1011 Tang H, Bomhoff MD, Briones E, Zhang L, Schnable JC, Lyons E. 2015. SynFind:  
 1012 compiling syntenic regions across any set of genomes on demand. *Genome*  
 1013 *Biol. Evol.* 7:3286–3298.
- 1014 Tausta SL, Coyle HM, Rothermel B, Stiefel V, Nelson T. 2002. Maize C<sub>4</sub> and non-C<sub>4</sub>  
 1015 NADP-dependent malic enzymes are encoded by distinct genes derived from a  
 1016 plastid-localized ancestor. *Plant Mol. Biol.* 50:635–652.
- 1017 Taylor L, Nunes-Nesi A, Parsley K, Leiss A, Leach G, Coates S, Wingler A, Fernie  
 1018 AR, Hibberd JM. 2010. Cytosolic pyruvate, orthophosphate dikinase functions in  
 1019 nitrogen remobilization during leaf senescence and limits individual seed growth  
 1020 and nitrogen content. *Plant J.* 62:641–652.
- 1021 Theissen G. 2001. Development of floral organ identity: stories from the MADS  
 1022 house. *Curr. Opin. Plant Biol.* 4:75–85.
- 1023 Theissen G, Saedler H. 2001. Plant biology. Floral quartets. *Nature* 409:469–471.

- 1024 Toledo-Ortiz G, Huq E, Quail PH. 2003. The *Arabidopsis* basic/helix-loop-helix  
1025 transcription factor family. *Plant Cell* 15:1749–1770.
- 1026 Valli A, Martin-Hernandez AM, Lopez-Moya JJ, Garcia JA. 2006. RNA silencing  
1027 suppression by a second copy of the P1 serine protease of *Cucumber vein*  
1028 *yellowing ipomovirus*, a member of the family *Potyviridae* that lacks the cysteine  
1029 protease HCPro. *J. Virol.* 80:10055–10063.
- 1030 Vicentini A, Barber JC, Aliscioni SS, Giussani LM, Kellog EA. 2008. The age of the  
1031 grasses and clusters of origins of C<sub>4</sub> photosynthesis. *Glob. Chang. Biol.*  
1032 14:2963–2977.
- 1033 Wang L, Czedik-Eysenberg A, Mertz RA, Si Y, Tohge T, Nunes-Nesi A, Arrivault S,  
1034 Dedow LK, Bryant DW, Zhou W, et al. 2014. Comparative analyses of C<sub>4</sub> and C<sub>3</sub>  
1035 photosynthesis in developing leaves of maize and rice. *Nat. Biotechnol.*  
1036 32:1158–1165.
- 1037 Wang Y, Bräutigam A, Weber APM, Zhu X-G. 2014. Three distinct biochemical  
1038 subtypes of C<sub>4</sub> photosynthesis? A modelling analysis. *J. Exp. Bot.* 65:3567–  
1039 3578.
- 1040 Williams BP, Aubry S, Hibberd JM. 2012. Molecular evolution of genes recruited into  
1041 C<sub>4</sub> photosynthesis. *Trends Plant Sci.* 17:213–220.
- 1042 Williams BP, Burgess SJ, Reyna-Llorens I, Knerova J, Aubry S, Stanley S, Hibberd  
1043 JM. 2016. An untranslated *cis*-element regulates the accumulation of multiple C<sub>4</sub>  
1044 enzymes in *Gynandropsis gynandra* mesophyll cells. *Plant Cell* 28:454–465.
- 1045 Yanagisawa S, Sheen J. 1998. Involvement of maize Dof zinc finger proteins in  
1046 tissue-specific and light-regulated gene expression. *Plant Cell* 10:75–89.